From Graphic Analysis of Equilibrium to Architectural Design. Cèsar Martinell

Cinta Lluis-Teruel, Josep Lluis i Ginovart

Abstract

Graphic statics is a structural calculation method derived from the concept of the thrust line and used by Catalan Modernism. A disciple of Antoni Gaudí, Cèsar Martinell, employed it in the design of 15 wineries between 1918 and 1922, which are now known as cathedrals of wine. One of them, the Pinell de Brai winery, illustrates the transformation of an initially projected structure with wooden trusses into one using masonry arches, which is the object of this study. By analyzing eight of the sketches using a graphic restitution methodology, it is possible to compare the masonry arches to the shapes of the catenary and the parabola, with an accuracy of ± 0.077 m for scale 1:100, and ± 0.052 m for scale 1:50. This analysis has made it possible to determine how the design process was developed: from trusses, to structural definition through trial and error using architectural drawing with graphic statics, and finally, the executed project featuring tied arches. In conclusion, none of the 14 drawn arches is strictly parabola or a catenary. The eight arches of the central nave tend toward the catenary shape, while the smaller-span arches of the side naves tend toward the parabola. The four masonry arches in the final project were drawn through point transposition using an auxiliary construction with a hanging chain, where the architectural structure was resolved using graphic methodologies.

Keywords: arches, catenary, graphic statics, Cèsar Martinell, parabola

Graphic statics and architectural design

Architectural structures were, for many years, the result of an experimental methodology until Robert Hooke (1635-1703) published *A description of helioscopes, and some other instruments*, in which he identified the ideal shape of an arch as the catenary curve [Hooke 1676, p. 31]. The scientific development of this curve was later addressed by Johann Bernoulli (1667-1748) in *Solutio problematis funicularii* [Bernoulli 1691] and Christiaan Huygens (1629-1695), in *Solutio eiusdem problematis* [Huygens 1691].
The mechanics of masonry structures conceptualized the thrust line as the locus of points through which internal forces pass within a system of given cutting planes [Huerta 2024], based on the mathematical foundations laid by Reverend Henry Moseley (1801-1872) [Moseley 1835].
This circumstance led to significant advances in graphic statics, which proved decisive for the architectural design of Catalan Modernism, particularly in the works of Rafael Guastavino Moreno (1842-1908) [Goodyear 1906] and Antoni Gaudí i Cornet (1852-1926) [Huerta 2006]. Both were trained in the concept of graphic transposition of structure into architectural design by Joan Torras Guardiola (1827-910) [Graus, Martin-Nieva 2015].
In addition to the Barcelona School of Architecture, established in 1875, the theory of ceramic vault construction also spread through the Architects' Association of Catalonia.

Fig. 1. Detail of the main beam of the Pinell de Brai Cooperative, built with brick arches. Image credit: Department of Culture of the Generalitat de Catalunya.

José Domènech i Estapà (1858-1917) suggested that parabolic shapes result from the equilibrium lines of a system with uniformly distributed loads, while catenary curves stem from the structure's self-weight [Domènech 1900]. Jaime Bayó Font (1873-1961) approached ceramic structures as flexible shells with different elastic coefficients in tension and compression [Bayó 1910]. Jeroni Martorell i Terrats (1876-1951) analyzed the use of iron tie-rods in masonry arches [Martorell 1910].
In structural science, the equilibrium conditions of a structure under a given load system can be analyzed using graphical statics, which employs the graphical representation of forces as vectors. Through this and with its adjustment, the architectural project can be produced, which is the subject of this paper. It is, therefore, a reflection on the relationship between structure and form, examined through the contribution of the graphic process and the skill involved in adjusting complex geometric forms using architectural drawing.
The study takes as a reference the figure of Cèsar Martinell i Brunet (1888-1973), a disciple and collaborator of Gaudí, who built 15 wineries between 1918 and 1922, known as cathedrals of wine, using graphic statics for the construction of their masonry arches. In the Historical Archive of the College of Architects of Catalonia in Barcelona ($COACAH_B$), the preliminary sketches (drawing C222-170) and the project (drawing H108I/18/170) for the Winery and Oil Mill of the Agricultural Cooperative of Pinell de Brai are preserved.

The building was constructed between 1918 and 1922 and has adjoining naves, one of which has two floors and is used as an oil mill, while the others are used as a wine cellar, where there is a structure formed by brick arches (fig. 1).
The analysis of the completed structure determined that none of the 28 arches defined by the function *f(a)* geometrically satisfy the equation of the catenary *f(c)*, nor that of the parabola *f(p)*. The fourteen smaller arches tend toward the parabolic function *f(p)*, while the larger-span arches tend toward the catenary function *f(c)* [Lluis i Ginovart et. al. 2017] (fig. 2).

Object of study and methodology

With knowledge of the completed work, the aim of this research is to analyze the evolution of the design process of the Pinell de Brai project through graphic documentation that served as the basis for the execution of the structure. The study focuses on the use of sketches to determine the masonry arches and to explore the relationship between structure and form through the following architectural drawings:

- H101I/6/reg. 2502: transverse section (0.606 x 0.390 m), graphite pencil on paper, scale 1:100;
- H103A/14/reg. 2290: transverse section (0.693 x 0.414 m), heliographic copy, scale 1:100;
- H103A/1/reg. 2293: detail of longitudinal and transverse sections (1.101 x 0.396 m), heliographic copy, scale 1:50;
- C222/170/1.1: detail of two central nave arches with graphic calculation (0.448 x 0.463 m), graphite pencil on paper, scale 1:50;
- C222/170/1.2: detail of two half-arch sections of the central nave with graphic calculation (1.025 x 0.491 m), graphite pencil on paper, scale 1:50;
- C222/170/1.5: transverse section (0.807 x 0.501 m), heliographic copy, scale 1:100;
- C222/170/2.4: detail of longitudinal and transverse section (1.378 x 0.498 m), graphite pencil on paper, scale 1:50;
- C222/170/2.6: detail of a central nave arch with graphic calculation (0.691 x 0.479 m), graphite pencil on paper, scale 1:50.

The methodological error in the trace restitution (*Ett*) depends on the drawing scale. It is determined as the sum of the precision of the original trace (*Ept*) (drawing

	Section A1				Section A2				Section A3				Section A4			
	A1.T1.a	A1.T2.b	A1.T3.c	A1.T4.d	A2.T1.a	A2.T2.b	A2.T3.c	A2.T4.b	A3.T1.a	A3.T2.b	A3.T3.c	A3.T4.d	A4.T1.a	A4.T2.b	A4.T3.c	A4.T4.d
Crown height	2,76	12,48	2,66	9,23	2,72	12,52	2,71	9,25	2,73	12,49	2,70	9,35	2,74	12,32	2,70	9,17
Span of the arch	2,91	13,55	2,87	10,10	2,89	13,57	2,82	10,07	2,89	13,59	2,84	10,08	2,91	13,53	2,84	9,99
f/l	0,95	0,92	0,93	0,91	0,94	0,92	0,96	0,92	0,95	0,92	0,95	0,93	0,94	0,91	0,95	0,92

	Section A5				Section A6				Section A7			
	A5.T1.a	A5.T2.b	A5.T3.c	A5.T4.d	A6.T1.a	A6.T2.b	A6.T3.c	A6.T4.d	A7.T1.a	A7.T2.b	A7.T3.c	A7.T4.d
Crown height	2,67	12,49	2,66	9,38	2,69	12,53	2,65	9,30	2,67	12,37	2,68	9,39
Span of the arch	2,88	13,58	2,81	10,09	2,87	13,59	2,81	10,07	2,89	13,54	2,82	10,09
f/l	0,93	0,92	0,95	0,93	0,94	0,92	0,94	0,92	0,92	0,91	0,95	0,93

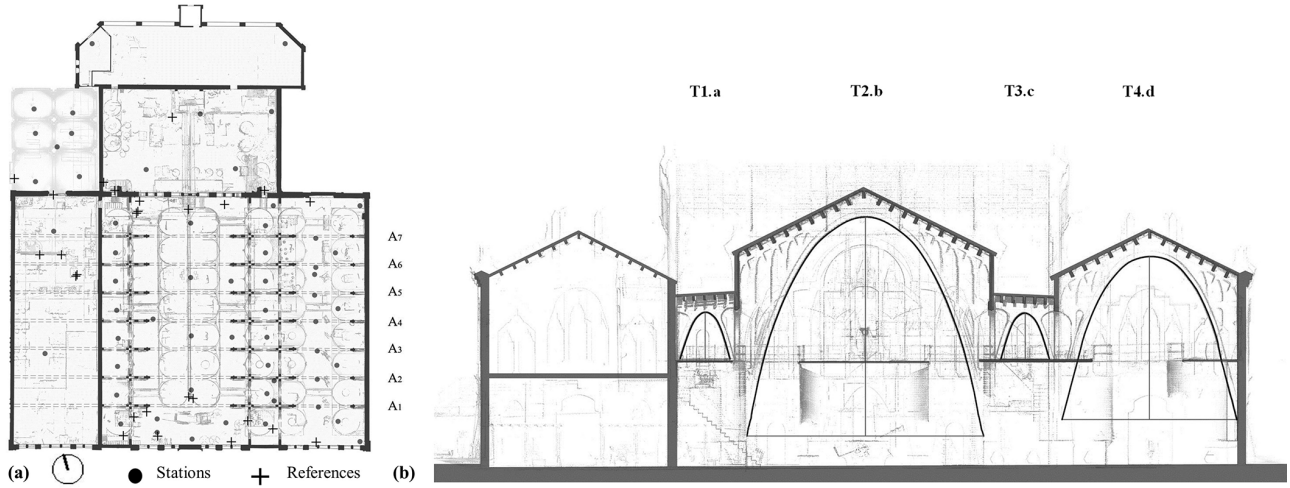

Fig. 2. Elevation (TLS) Sindicato Agrícola de Pinell de Bray. Leica Scan Station P40 (2015). Units of length expressed in meters.

H1011/6/reg. 2502), in which 13-dimension lines were noted and used as the basis for calibration, resulting in a root mean square error of 0.001, with a tolerance of ± 0.026 m defined as *TTi.i*. The pixel reference of a graphite line at scale *Elt*, (1:100 = ± 0.041 m) and (1:50 = ± 0.021 m), and the estimated digital restitution error is considered as *Eit* (1:100 = ± 0.010 m) and (1:50 = ± 0.005 m):

$$Ett = \Sigma\ (Ept, Elt, Eit) \qquad (1)$$

The resulting errors are Ett_{100} = ± 0.077 m and Ett_{150} = ± 0.052 m, taking the measurement of the smallest arch as a reference (*TTa.1* and *TTc.3*) *l* = 2.650 m.

$$Ett_{100} = \pm\ 2.906\%;\ Ett_{150} = \pm\ 1.962\%$$

The nomenclature for the executed arches is: (*T1.a*, *T1.b*, *T1.c*, *T1.d*); for the project arches: (*Ta.1*, *Tb.2*, *Tc.3*, *Td.4*). The graphic construction of the arches is based on the theoretical dimensions established through the drawn measurements of the trace (drawing H1011/6/reg. 2502), which are taken as the theoretical references (*TTa.1*, *TTb.2*, *TTc.3*, *TTd.4*). The differences between them are not significant in terms of the rise *(f)* and the span (*l*).

Methodology for the graphic comparison of the curve traces

The graphic verification is carried out using the functions of the parabola and the catenary, where *p* represents the weight per unit length of a hanging element, and T_o minimum horizontal tension:

$$f(p) = p\,\frac{x^2}{2T_0} \qquad (2)$$

$$f(c) = T_0/p.\,Cos\,h\left(\frac{x.p}{T_0}\right) \qquad (3)$$

The process is carried out within a Cartesian coordinate system (*x*, *y*), where the coordinates (*x* = *l*) and (*y* = *f*) represent the span and the rise, respectively. Ten points are defined per branch for both figures, distributed along the *x*-axis, allowing the establishment of *(lcx)* and *(lpx)*, similar to those used in funicular polygons. The parabola is drawn by knowing the vertex, the axis, and the springing points, using projective bundles over a parallelogram (*f*, *l*/2) divided into 10 segments. The catenary is determined using 10 points, whose projection follows a similar projective sequence (*yci*/*n*). Considering that, when the coordinates (*yci* = *ypi*) of the catenary *f(c)* and the parabola *f(p)* are equal, the coordinates *xci* are always greater than *xpi*. In this way, it is possible to verify the projective difference (*xci* - *xpi*) between the catenary *f(c)* and the parabola *f(p)* (fig. 3).

The difference depends on the drawing scale and on the ratio between the rise and the span of the arch. Verification is carried out by constructing a canonical reference (10 m), which corresponds to the average span of the arches in the project. In this way, it is observed that the smaller the rise-to-span ratio, the more similar the two curves become. The greatest distortions between the widths of the two figures occur in interval [7], which corresponds to the projection between 30% and 40% from the springing points (l_1, l_2).
Thus, for rise/span ratios (*f*/*l*: 0.25, 0.50, 0.75, 1.00), the corresponding differences (*xci* - *xpi*) are: 0.069 m, 0.194 m, 0.313 m, 0.414 m.
In delineation, these canonical curves yield values of: [*E*: 1/100 (*xci* - *xpi*) = 0.000 m, 0.002 m, 0.003 m, 0.004 m], while [*E*: 1/50 (*xci* - *xpi*) = 0.001 m, 0.004 m, 0.006 m, 0.008 m]. Similar results are found in the theoretical arches (drawing H1011/6/reg. 2502) (*TTa.1*, *TTb.2*, *TTc.3*, *TTd.4*), with differences in the built work of 0.115 m, 0.469 m, 0.396 m, and 0.414 m respectively.

(a) Difference between canonical functions f(c)-f(p)

Rise/Span		0,25	0,5	0,75	1,00
Stretch	Interval				
V	1	0,000	0,000	0,000	0,000
1/10x(l/2)	2	0,027	0,067	0,102	0,127
2/10x(l/2)	3	0,040	0,106	1,666	0,213
3/10x(l/2)	4	0,047	0,145	0,227	0,299
4/10x(l/2)	5	0,061	0,175	0,278	0,370
5/10x(l/2)	6	0,069	0,194	0,313	0,414
6/10x(l/2)	7	0,070	0,198	0,375	0,426
7/10x(l/2)	8	0,065	0,185	0,301	0,400
8/10x(l/2)	9	0,052	0,150	0,243	0,326
9/10x(l/2)	10	0,031	0,009	0,17	0,196
l/2	11	0,000	0,000	0,000	0,000

(b) Difference between theoretical arches f(c)-f(p)

Rise/Span		TTa.1	TTb.2	TTc.3	TTd.4
Stretch	Interval				
V	1	0,000	0,000	0,000	0,000
1/10x(l/2)	2	0,034	0,151	0,127	0,127
2/10x(l/2)	3	0,058	0,245	0,205	0,213
3/10x(l/2)	4	0,083	0,342	0,285	0,299
4/10x(l/2)	5	0,099	0,419	0,354	0,370
5/10x(l/2)	6	0,115	0,469	0,396	0,414
6/10x(l/2)	7	0,119	0,482	0,407	0,426
7/10x(l/2)	8	0,111	0,451	0,382	0,400
8/10x(l/2)	9	0,091	0,365	0,311	0,326
9/10x(l/2)	10	0,053	0,202	0,187	0,196
l/2	11	0,000	0,000	0,000	0,000

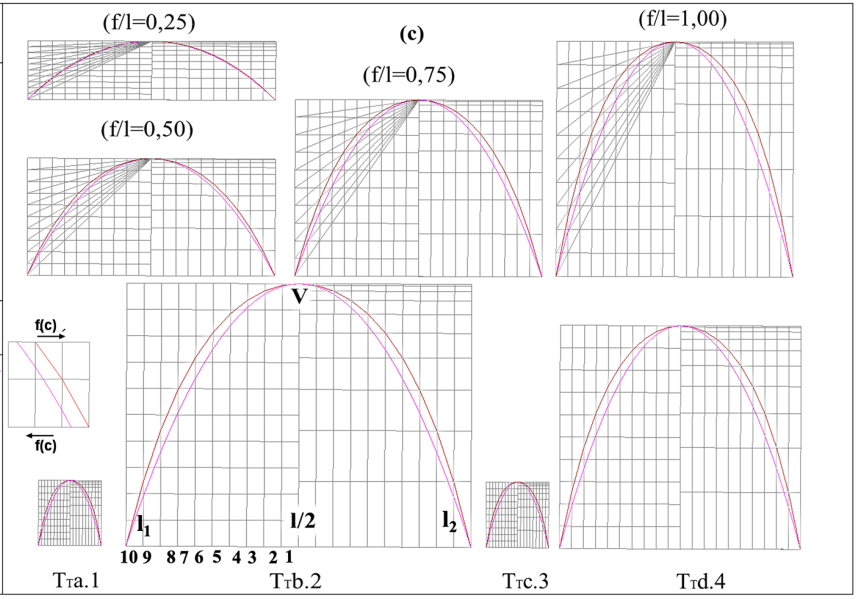

Fig. 3. Relationship between the shapes of the masonry arches and the functions of the catenary f(c) and the parabola f(p). Units of length expressed in meters, referring to a standard of 10 m arc length.

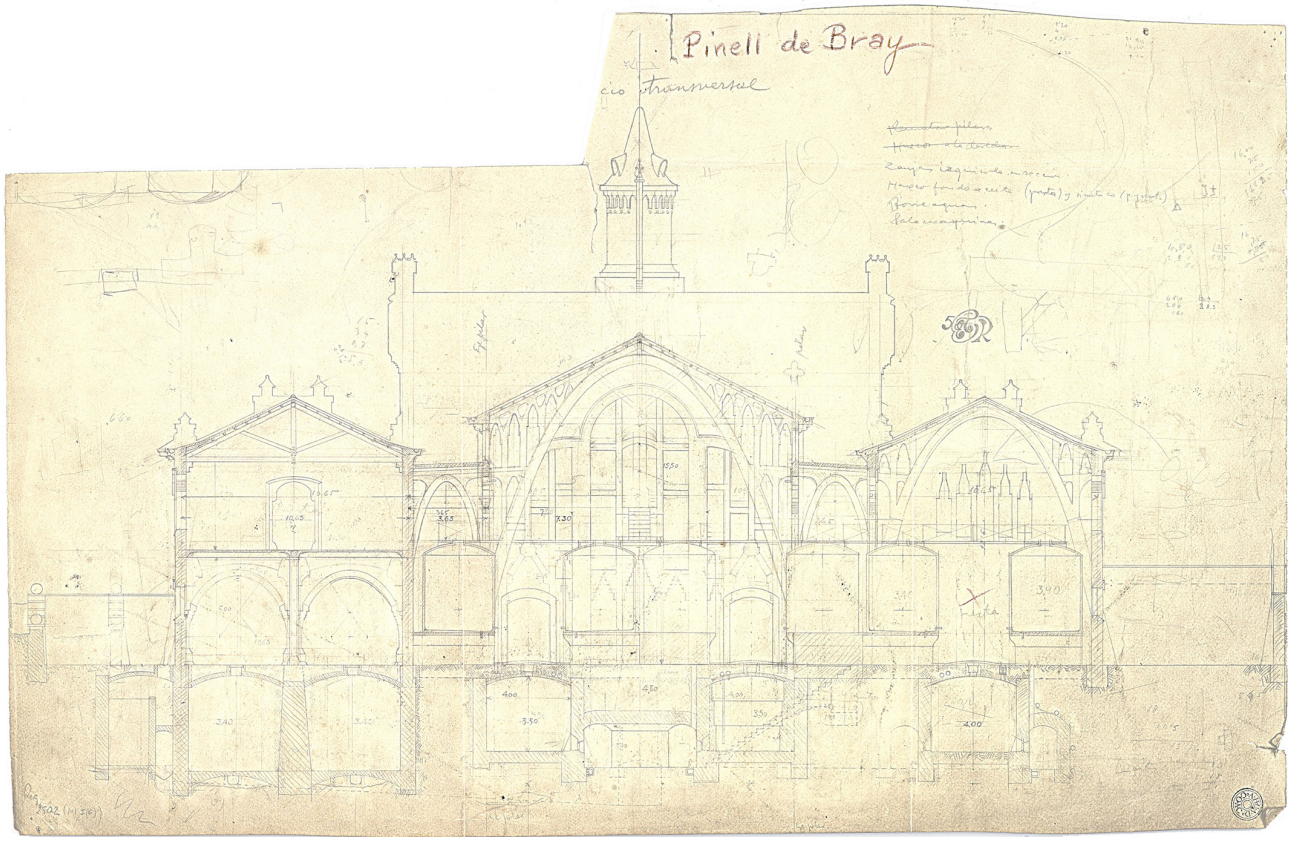

Fig. 4. Trace of drawing H101I/6/reg. 2502 as the basis for project (P1) (drawing C222/170/1.5) and (P2) (drawing H103A/14/reg. 2290). Image credits: COAC AH_B Archive.

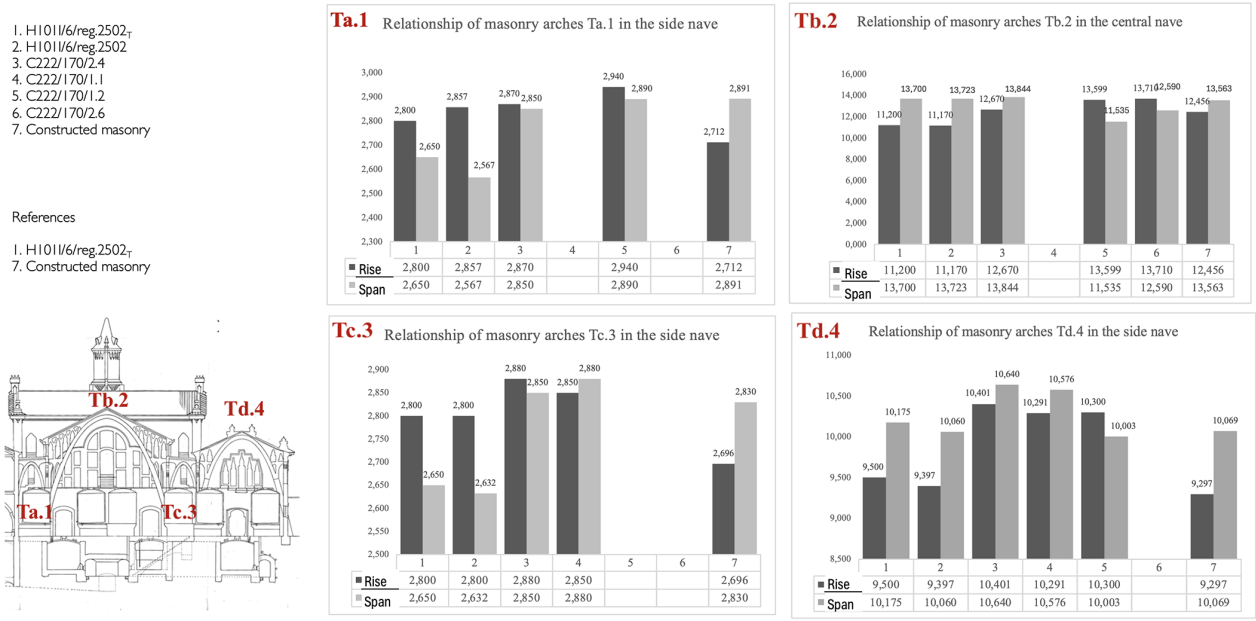

Fig. 5. Design trials of the masonry arch dimensions with reference to the theoretical levels of the initial project (1. H1011/6/reg. 2502T) and to the executed work (7. constructed masonry). Units of length expressed in meters.

Initial modification of the project: drawing C222/170/1.5

In the transverse section (drawing C222/170/1.5), all three naves are covered with wooden trusses, and this is considered the original design *P1*. A correction made in strong graphite is visible in the basement area, adapting it to the topography. Additionally, very fine graphite lines appear beneath two of the trusses, indicating their replacement by masonry arches. In project (drawing H103A/14/reg. 2290), the nave designated for the oil mill retains its original truss structure, while the two intended for the winery are constructed with four masonry arches. Moreover, the ground floor section shows clear adaptation to the existing topography and is regarded as the foundation of the new design *P2*. Both traces share a common base, i.e. the matrix (H1011/6/reg. 2502) (fig. 4) where the superposition of both proposals can be observed the trusses from the initial project (C222/170/1.5) and the masonry arches from drawing H103A/14/reg. 2290. This sketch preserves the section of the basement level from design (*P1*), which would later be modified in the final project (*P2*).

The shortage of wood and steel resulting from the First World War, along with the financial constraints of the cooperatives, led to the replacement of the roof trusses with brick masonry arches [Llorens 2013]. According to the construction budget, the common brick was to be sourced from Benissanet and Tortosa; the facing brick from Mora; and the molded brick from Reus all of which are nearby towns (drawing C 222/170).

Later modifications and the use of graphic statics for design trials

The design change led to a dimensioning process using funicular polygons for the four arches. When referencing the dimensions of those with annotated measurements

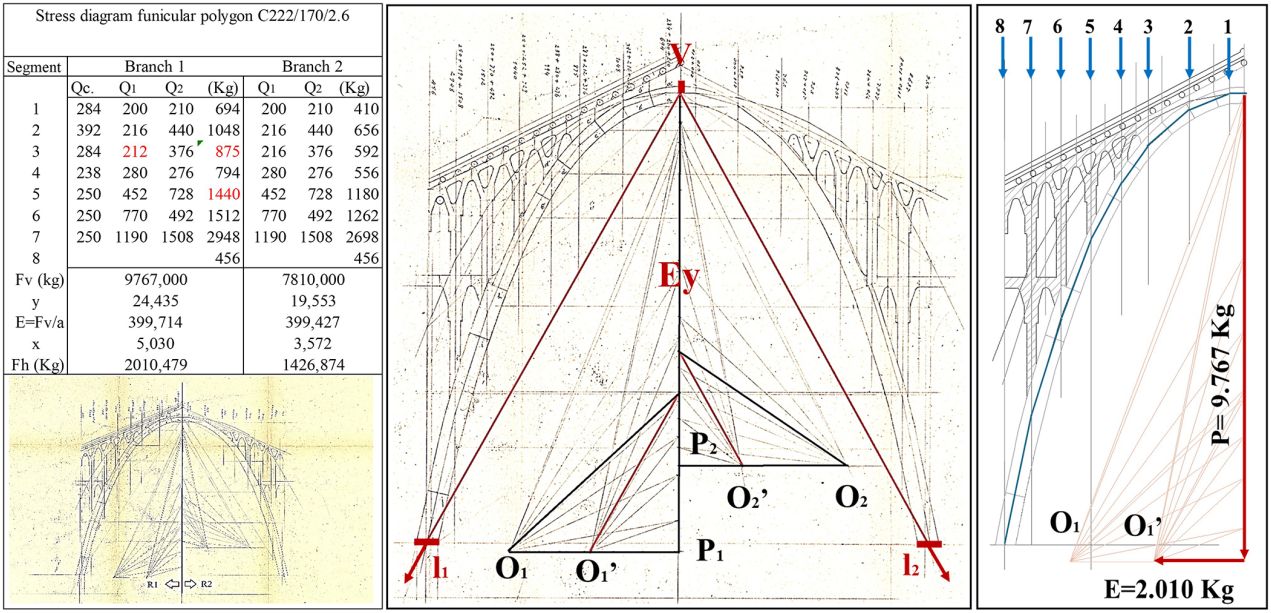

Stress diagram funicular polygon C222/170/2.6

Segment	Branch 1				Branch 2		
	Qc.	Q1	Q2	(Kg)	Q1	Q2	(Kg)
1	284	200	210	694	200	210	410
2	392	216	440	1048	216	440	656
3	284	212	376	875	216	376	592
4	238	280	276	794	280	276	556
5	250	452	728	1440	452	728	1180
6	250	770	492	1512	770	492	1262
7	250	1190	1508	2948	1190	1508	2698
8				456			456
Fv (kg)	9767,000				7810,000		
y	24,435				19,553		
E=Fv/a	399,714				399,427		
x	5,030				3,572		
Fh (Kg)	2010,479				1426,874		

Fig. 6. Funicular polygons of masonry arches Tb.2 (drawing C222/170/2.6). Units of length expressed in meters. Image credits: COAC AH$_B$ Archive.

(drawing H1011/6/reg. 2502T), differences in all dimensions can be observed. In this way, the design trial (drawing C222/170/1.1) increases both the rise (*f*) and span (*l*) of arches *Tc.3* and *Td.4*. In drawings C222/170/1.2 and C222/170/2.6, both the rise and span are increased for arch *Ta.1*, and the rise is also increased for *Tb.2* (fig. 5).
Develop some preliminary layouts before the final solution, forming two funicular polygons for *Tb.2* and *Tc.3* in drawing C222/170/1.1, two more for arches *Tb.2* and *Td.4* in drawing C222/170/1.2, and another one for *Tb.2* in drawing C222/170/2.6.
Each masonry arch operates with two branches (R_1, R_2). In R_1, the self-weight and the load of the upper finish (Q_1, Q_2) are applied, along with the live load of the roof (Qc_1) while R_2 includes only Q_1 and Q_2 (fig. 6a). The funicular is constructed using eight segments of the arch, with the line passing through the center of the core of the elastic section. The resultant used to determine the thrust *E* is constructed with a triangle located at the center of the section, with vertex *V*, and at the springing point of the arch I_1 and I_2, aligned along a central axis *Ey*. A provisional pole is drawn for each branch, O_1 and O_2, followed by the final poles O_1' and O_2' (fig. 6b). The resulting vertical component *P* is the sum (P_1 - *8*), and the horizontal component is (*P* - *O'*) (fig. 6c).
The tests show that the arches in the naves are segmental ($f/l > 1$), whereas in the initial project they were lowered ($f/l < 1$), and therefore, the trials would result in a thrust *E* smaller than that of drawing H1011/6/reg. 2502_T.
The analysis of the curves traced for the masonry arches is carried out by dividing the curve into two branches along the vertical axis that passes through the vertex (*V*), where the half-span ($l/2$) is divided into ten segments ($xa_{1\text{-}10}$) determining ($ya_{1\text{-}10}$). This point serves as a reference to determine the measurement differences with respect to the parabola and the catenary:

$$(ya_{1\text{-}10}) = (yp_{1\text{-}10}) = (yc_{1\text{-}10}) \quad (4)$$

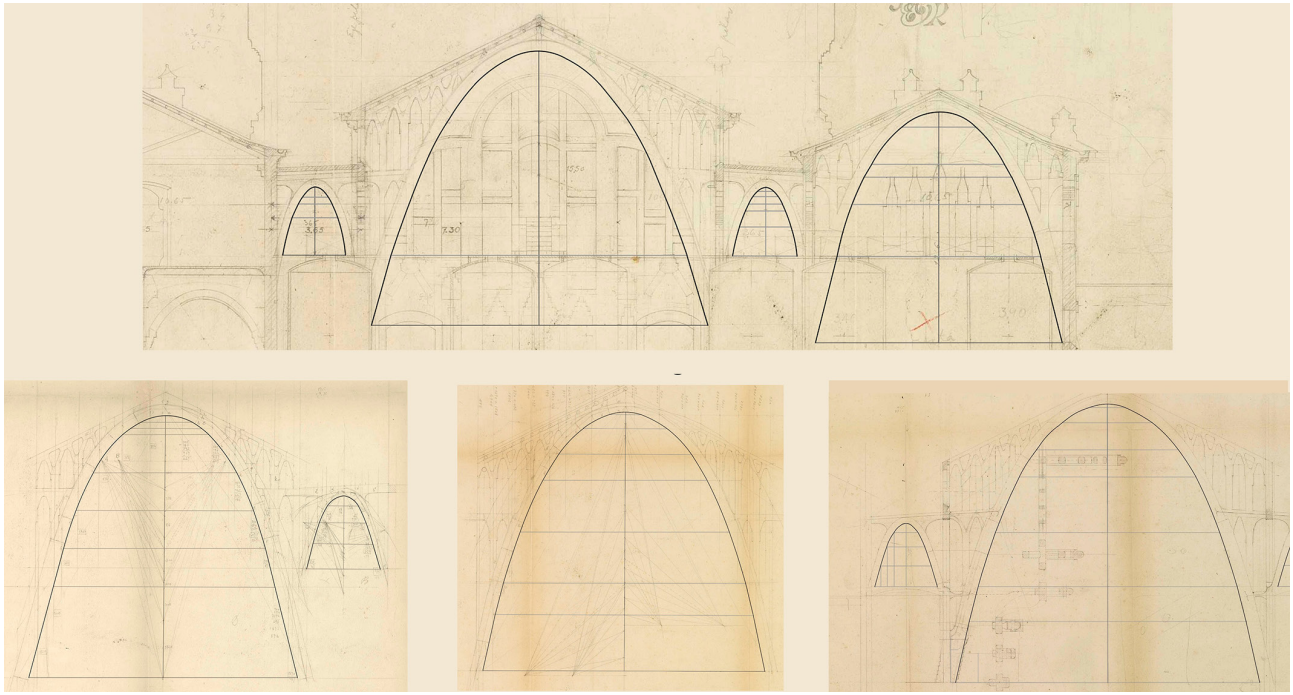

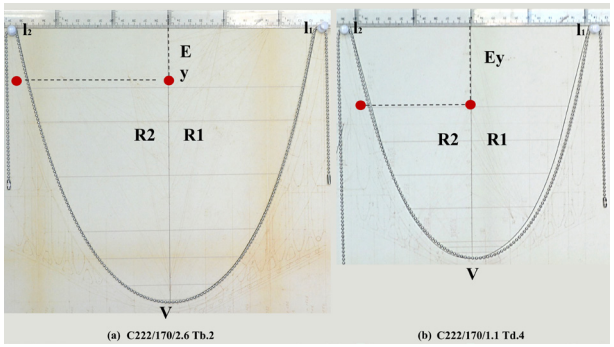

Fig. 7. Detail of the alignment lines in the trace of the masonry arches. Image credits: COAC AH$_B$ Archive.

Fig. 8. Verification of the geometric traces of the arches using an inverted chain.

In this way, the following is established:

$$dp = (xa_{1\text{-}10} - xp_{1\text{-}10});\ dc = (xa_{1\text{-}10} - xc_{1\text{-}10}) \qquad (5)$$

It is observed that the layout of the two branches R_1 and R_2 is not exactly symmetrical, and that none of the fourteen curves correspond exactly to *f(xc)* catenaries or *f(p)* parabolas. Of the 144 points analyzed from the eight arches of the central naves (*Tb.2*, *Td.4*), 12.50% of the points (*f(p)*) approximate the parabola, while 87.50% (*f(c)*) tend toward the catenary. Of the 100 points from the arches of the side naves (*Ta.1*, *Tc.3*), 75.00% (*f(p)*) approximate the parabola, while 25.00% (*f(c)*) tend toward the catenary. In the tracing of the curves, certain points are marked in graphite along the curve's axis and are transferred perpendicularly toward branch R_2 of the curve, located to the right of the drafter. This suggests that the function *f(a)* was drawn using a point transposition method (fig. 7).

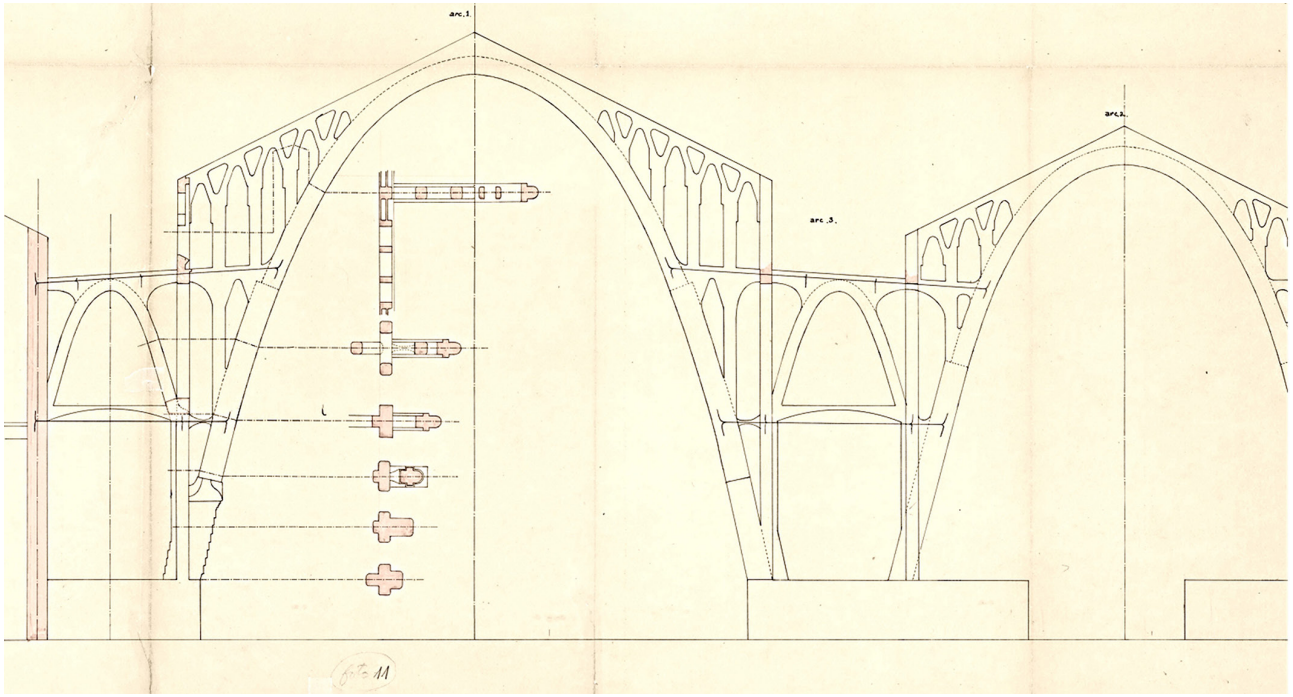

Fig. 9. Details of the anchors in the final section of the modified project (drawing H103A/11reg. 2293). Image credits: COAC AH$_B$ Archive.

P	AC22/170/2.4.a.1						AC22/170/2.4.b.2						AC22/170/2.4.c.3						AC22/170/2.4.d.4					
	(x0-xi)	y	Δ(x0-xi)	Δy	%Δx	%Δy	(x0-xi)	y	Δ(x0-xi)	Δy	%Δx	%Δy	(x0-xi)	y	Δ(x0-xi)	Δy	%Δx	%Δy	(x0-xi)	y	Δ(x0-xi)	Δy	%Δx	%Δy
1	5,700	0,000	0,000	1,880	1,000	0,000	27,700	0,000	0,000	5,770	1,000	0,000	5,700	0,000	0,000	1,920	1,000	0,000	21,280	0,000	0,000	7,210	1,000	0,000
2	4,580	1,880	1,120	1,730	0,804	0,328	25,200	5,770	2,500	2,960	0,910	0,228	4,630	1,920	1,070	1,690	0,812	0,334	17,630	7,210	3,650	1,520	0,828	0,347
3	3,410	3,610	1,170	1,310	0,598	0,629	23,580	8,730	1,620	4,930	0,851	0,345	3,470	3,610	1,160	1,310	0,609	0,628	16,860	8,730	0,770	1,910	0,792	0,420
4	2,180	4,920	1,230	0,820	0,382	0,857	20,410	13,660	3,170	5,050	0,737	0,539	2,240	4,920	1,230	0,830	0,393	0,856	15,750	10,640	1,110	2,600	0,740	0,512
5	0,000	5,740	2,180	0,000	0,000	1,000	16,090	18,710	4,320	2,460	0,581	0,739	0,000	5,750	2,240	0,000	0,000	1,000	14,120	13,240	1,630	3,920	0,664	0,637
6							12,880	21,170	3,210	2,460	0,465	0,836							10,360	17,160	3,760	2,120	0,487	0,825
7							8,140	23,630	4,740	1,390	0,294	0,933							6,980	19,280	3,380	0,510	0,328	0,927
8							3,160	25,020	4,980	0,310	0,114	0,988							5,800	19,790	1,180	0,490	0,273	0,951
9							0,000	25,330	3,160	0,000	0,000	1,000							4,220	20,280	1,580	0,520	0,198	0,975
10																			0,000	20,800	4,220	0,000	0,000	1,000

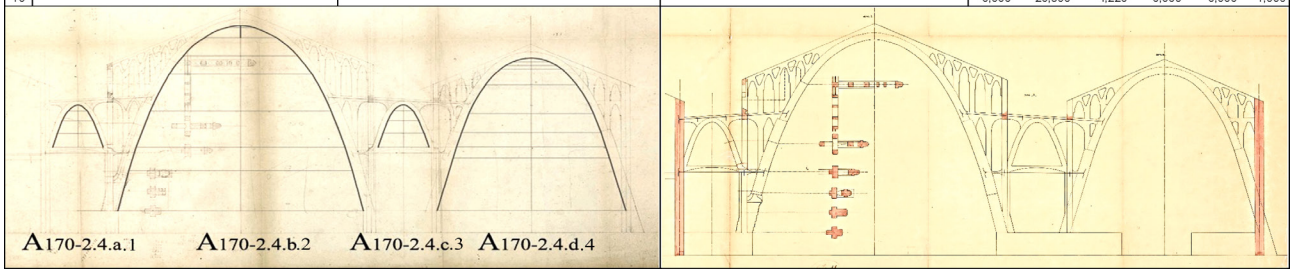

Fig. 10. Determination of the singular points in the tracing of the masonry arches.

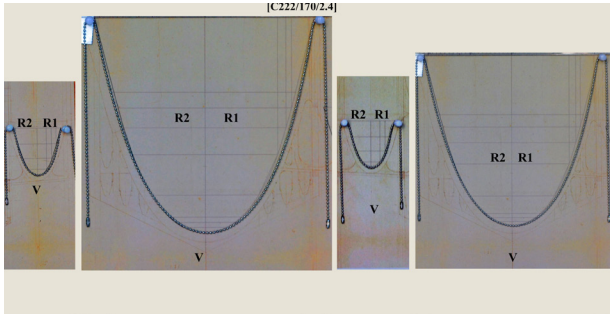

Fig. 11. Verification of the geometric traces of the arches using an inverted chain.

A verification was carried out to determine the geometry of the traced curve by superimposing a chain with 320 beads per linear meter, weighing 8.059 grams, measured using a Mettler Toledo balance (PB303-S Delta Range). The setup was documented through photographs taken with a Nikon Digital Camera D5200, equipped with a Nikon DX SWN VR Aspherical (∞-0.28 m/0.92 ft Ø 52). It was observed that the transposition of measurements is performed along the vertical axis *Ey* and transferred onto branch R_2, located to the right of the trace. Furthermore, there is a high degree of alignment in the points of branch R_2 (fig. 8a, b), whereas the symmetry in branch R_1 of the curve is not always consistent (fig. 8b).

The definition of the project: drawing C222/170/2.4 and H103A/1/reg. 2293

With the alignments, the base for the final project is established, using the trace that defines the geometry of the arches in the transverse section, with six sections perpendicular to the cut, and with the details of the upper arcade (drawing C222/170/2.4). It also includes the first three bays of the longitudinal section, where auxiliary lines appear for drawing the masonry arches, as well as notes with numerical operations, though no funicular analysis is present. In

the heliographic copy H103A/1/reg. 2293, the arches are numbered, and the anchoring of the ties from the central nave arches to those of the side naves is highlighted, taking advantage of the floor slab (fig. 9).
The tracing of the arches is carried out through the transposition of measurements, and it is observed that there is no orderly sequence in the progression of the abscissas Δy. There is a convergence of auxiliary traces for arches *Ta.1*, *Tc.3*, and *Td.4* within the interval 0.629%-0.637% from the springing points I_1 *and* I_2, which is drawn with a straight line. This part of the curve is where *f'(a)* reaches its maximum slope. The point of minimum curvature in all the arches appears in the segment 0.825%-0.857%, and the vertex *V* is located where *f'(a)* = 0 (fig. 10). In the verification using a chain, a high degree of alignment is observed with branch R_2 of the traces of the four arches, which is where the transposition of measurements occurs (fig. 11).
On the other hand, when comparing the tracing parameters with those of the parabola and the catenary, it is observed that the dimensional results of *Ta.1* and *Tc.3* approximate the parabola, while *Tb.2* and *Td.4* tend toward the catenary. As for the lengths of the four arches, all of them fall within the methodological error range E_{tt150} = ± 1,962% of the catenary function (fig. 12).
In the geometry of the trace *Tb.2*, an increase of 1.470 m in the rise of the arch is noted compared to the original design H101I/6/reg. 2502T, while the span increases by only 0.144 m. As a result, its section is more elevated, and therefore its thrust *E* will be lower. The dimensions of this arch are close to those of the executed work (*f*, *l* = + 0.214, + 0.281 m) and the ratio is very similar (*f/l*, 0.915, 0.918).
The dimensions of the as-built arch *T4.d* are close to the *Td.4* of the initial project and differ from the modified drawing *C222/170/2.4*. The geometry of *Ta.1* and *Tc.3* is very similar to the original design, the modified design, and the actual construction.

Conclusion

It has been possible to determine how the design process was developed, with the structural definition carried out

	AC22/170/2.4.a.1					AC22/170/2.4.b.2				
	(x0-xi)	y	Δ(x0-xi)	Δy	%Δx %Δy	(x0-xi)	y	Δ(x0-xi)	Δy	%Δx %Δy
Lf (xa) m			6,668					30,507		
L f(xp) m			6,653					30,071		
L f(xc) m			6,795					30,667		
L f(xp)- L f(xa) m	0,015			0,225	%	0,436			1,429	%
L f(xc)- L f(xa) m	-0,127			-1,905	%	-0,160			-0,524	%
Sf (xa) m^2			5,424					124,287		
S f(xp) m^2			5,451					116,990		
S f(xc) m^2			5,909					125,981		
S f(xp)- S f(xa) m^2	-0,027			-0,498	%	7,297			5,871	%
S f(xc)- S f(xa) m^2	-0,485			-8,942	%	-1,694			-1,363	%

	AC22/170/2.4.c.3					AC22/170/2.4.d.4				
	(x0-xi)	y	Δ(x0-xi)	Δy	%Δx %Δy	(x0-xi)	y	Δ(x0-xi)	Δy	%Δx %Δy
Lf (xa) m			6,684					24,708		
L f(xp) m			6,674					24,289		
L f(xc) m			6,813					24,783		
L f(xp)- L f(xa) m	0,010			0,150	%	0,419			1,696	%
L f(xc)- L f(xa) m	-0,129			-1,930	%	-0,075			-0,304	%
Sf (xa) m^2			5,443					77,793		
S f(xp) m^2			5,473					73,770		
S f(xc) m^2			5,931					79,783		
S f(xp)- S f(xa) m^2	-0,030			-0,551	%	4,023			5,171	%
S f(xc)- S f(xa) m^2	-0,488			-8,966	%	2,000			2,571	%

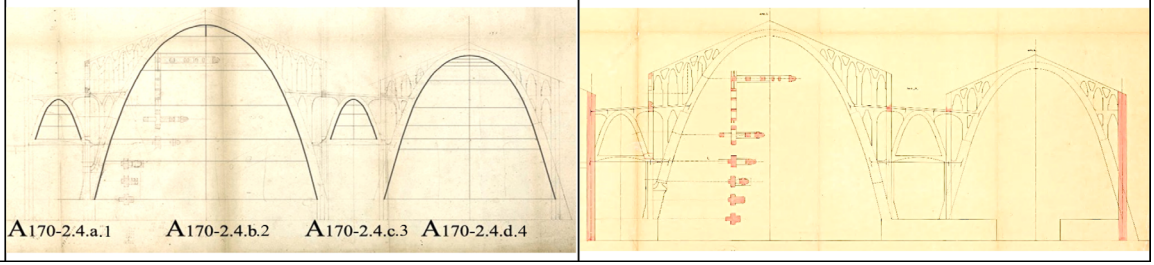

Fig. 12. Dimensional comparison of the arches with respect to the parabola and catenary.

through a graphic sequence: initial trusses, design trials of the arches using graphic statics, and the final project with tied arches. The executed work reflects the original geometry of arches *Ta.1*, *Tc.3*, and *Td.4*, as well as the increased rise of *Tb.2*. None of the 14 drawn arches corresponds strictly to a parabolic or catenary function. The eight arches in the central naves tend toward the catenary, while those with smaller spans in the side naves tend toward the parabola although all remain within the methodological margin of error for catenary restitution. The four masonry arches in the final project were drawn using point transposition, carried out through an auxiliary construction made with a hanging chain. Martinell relies on this simulation because it allows him to graphically plot a curve to draw the arches of the structure in a simpler way than plotting a parabola. The architectural structure was resolved using vector-based graphic methodologies, and its form was defined through the transposition of architectural drawing demonstrating the representational power of drawing in determining the structure of the architectural project.

Abbreviations and nomenclature

$COACAH_B$: Collegi Oficial Arquitectes Catalunya, Arxiu Històric Barcelona.
$COACAH_{To}$: Collegi Oficial Arquitectes Catalunya, Arxiu Històric Tortosa.
(f): rise of arches.
f(a): geometric function of masonry arches.
f(c): catenary function.
f(p): parabolic function.
(l): span of arches.
T1.a, *T1.b*, *T1.c*, *T1.d*: arches actually built on site.
Ta.1, *Tb.2*, *Tc.3*, *Td.4*: arches in the architectural project.

Authors

Cinta Lluis-Teruel, School of Architecture, Universitat Internacional de Catalunya, cintalluis@uic.es
Josep Lluis i Ginovart, School of Architecture, Universitat Internacional de Catalunya, jlluis@uic.es

Reference List

Bayó, J. (1910). La bóveda tabicada. In *Anuario de la Asociación de Arquitectos de Cataluña,* pp. 157-184.

Bernoulli, J. (1691). Solutio problematis funicaularii exhibita a Johanne Bernoulli. In *Actae Eruditorum*, pp. 274-276. <https://gallica.bnf.fr/ark:/12148/bpt6k500093/f286.item> (accessed 9 February 2026).

Domènech, J. (1900). La fábrica de ladrillo en la construcción catalana. In *Anuario de la Asociación de Arquitectos de Cataluña*, pp. 37-48.

Goodyear, W.H. (1906). The Columbia University Chapel. In *The Brickbuilder*, vol. 15, pp. 261-269, Plates 162-168.

Graus, R., Martin-Nieva, H. (2015). The beauty of a beam: The continuity of Joan Torras's beam of equal strength in the work of his disciples Guastavino, Gaudí, and Jujol. In *International Journal of Architectural Heritage*, Vol. 9, No. 4, pp. 341-351.

Hooke, R. (1676). *A description of helioscopes, and some other instruments*. London: Printed by T.R. for John Martyn.

Huerta, S. (2006). Structural Design in the Work of Gaudí. In *Architectural Science Review*, Vol. 49, No. 4, pp. 324-339. DOI: 10.3763/asre.2006.4943.

Huerta, S. (2024). El análisis gráfico de equilibrio de arcos, bóvedas y edificios: Un esquema de su desarrollo histórico. In *Revista de la Construcción*, Vol. 4, pp. 1-42. DOI: 10.4995/rdhc.2024.23120.

Huygens, C. (1691). Christiani Hugenii, Dynastae in Zulechem, Solutio eiusdem problematis. In *Actae Eruditorum*, pp. 281-290. <https://gallica.bnf.fr/ark:/12148/bpt6k500093/f295.item> (accessed 9 February 2026).

Llorens, J.I. (2013). Wine cathedrals: Making the most of masonry. In *Construction Materials*, Vol. 166, No. 6, pp. 329-342. DOI: 10.1680/coma.12.00023.

Lluis i Ginovart, J., López Piquer, M., Costa, A., Coll, S. (2017). Design and layout of arches in Pinell de Brai cooperative. The legacy of Catalan construction on Cèsar Martinell wine cellar designs (1919-1927). In *Construction History International*, Vol. 32, No. 2, pp. 67-82. <https://patriarq.wordpress.com/wp-content/uploads/2018/03/2017-lluis-et-al-design-and-layout-of-arches-in-pinell-de-brai-cooperative_ch.pdf> (accessed 19 November 2025).

Martorell, J. (1910). Estructuras de ladrillo y hierro atirantado en la arquitectura catalana moderna. In *Anuario de la Asociación de Arquitectos de Cataluña*, pp. 119-146.

Moseley, H. (1835). On the equilibrium of the arch. In *Cambridge Philosophical Transactions*, Vol. 5, pp. 293-313.